EARTH'S CRYOSPHERE
SCIENTIFIC JOURNAL

Earth`s Cryosphere, 2018, vol. XXII, No. 2, pp. 44–53 **http://earthcryosphere.ru/**

RELIABILITY OF BASEMENTS AND STRUCTURES IN CRYOLITHOZONE

DOI: 10.21782/EC2541-9994-2018-2(44-53)

METHOD OF CALCULATION OF AXIAL LOAD ON THE WELLBORE CASING DURING THAWING OF FROZEN HOST SEDIMENTS

J.B. Gorelik, P.V. Soldatov

Earth Cryosphere Institute, Tyumen Scientific Centre SB RAS,
P/O box 1230, Tyumen, 625000, Russia; gorelik@ikz.ru

The paper presents data on casing deformations reported from high-latitude hydrocarbon production fields, and results of their comparison with laboratory simulations of a casing subjected to axial compression leading to deformations, such as buckling, similar to those occurring under operation conditions. The frozen soils in regions of well placements with reported buckled casings include epigenetically frozen clayey layers. In the thawed state, such layers have better mechanical properties and may retain their integrity under significant loads. As such, the thawed part of the layer comprises three supporting elements: wellbore casing; its own extension into the frozen soils; and the underlying thawed soils. A method for calculating axial loads on the casing depending on the thawed area size and thawing soils properties is proposed. The axial load exerted on casing tends to grow reaching its maximum at the initial stages of well operation, and then decreases to the asymptotically constant value (regardless of thaw radius). Early years of well operations appear to be most hazardous for the constructions, which agrees well with the known practical results.

Frozen soils, thawed soils, casing, axial loads, wellbore casing buckling

INTRODUCTION

Construction and operation of wells in hydrocarbon fields in permafrost areas are challenged by certain risks associated with additional loads on wellbore casing caused by freeze/ thaw of host sediments [*Goodman, 1978; Medvedskiy, 1987; Hirshberg et al., 1988; Bykov, 1991; Vyakhirev, 1996; Remizov et al., 2001; Vasilevsky, 2002*].

Permafrost thawing caused by the warming effect of a well is associated with negative friction forces due to the partially sticking thawed soils onto the exterior wall of the casing whose motion is directed along the longitudinal axis of the wellbore. The magnitude of these forces controlled primarily by the radius of thawing (thaw radius) and the thickness of thawed formation [*Bratsev and Zhukov, 1965*] can reach a critical value for certain depths, causing the loss of axial stability (buckling) of the wellbore casing, even in case of sustained lateral support from the unfrozen soils [*Gorelik and Soldatov, 2016*].

Another type of hazardous impact from axial load is plastic deformation of the casing material of pipe and production string observed as bulging near the coupling connections, which can also lead to depressurization of the latter and failure of wellbore casing and, ultimately, to forced shutdown of wells [*Hirshberg et al., 1988*]. The type and consequences of such deformations are considered here in greater detail and illustrated by the examples.

1. Factual data on wellbore casing deformations and their laboratory simulations

1.1. The Yamburg GC field. The mode of deformation of two wells at the Yamburg gas condensate field (GCF) complete with other data is discussed in detail in [*Gorelik and Soldatov, 2016*]. A brief account of the design and deformations of these wells are given below, with Table 1 providing data on their configuration within the permafrost interval and some technological parameters. Table 2 provides inclination measurements for the deformed segment of casing and its position in the vertical section of Well 8032. Figure 1, *b* represents the mode of deformation in this segment of the wellbore casing, indicating the loss of its axial stability, which accounts for be one half-wave curvature under the conditions of sustained lateral support from unfrozen soils (the wellhead subsidence measured 0.66 m).

Deformations of the second well (Well 8033) amassed near the coupling connections, exhibit a different pattern and are shown in Fig. 1, *a*. The figure also shows the buckling intervals and relative position of the two deformed wells with respect to each other in the section along the axial line of the well pad.

The pulse flaw-detection method has revealed a rupture with displacement on the coupling connection surface in the casing string of Well 8033 (Fig. 1, *a*), with the pipe however retaining its vertical position

Table 1. **Technological and design parameters of the deformed wells, the Yamburg GCF**

Well	$D \times s$		Well drilling period	Commissioning date	Shutdown date
	Conductor (surface casing)	Production string			
8032	245 × 11.1	168.3 × 8.94	22.12.1994–08.01.1995	24.03.1996	01.05.1997
8033	245 × 11.1	168.3 × 8.94	14.01.1995–08.02.1995	24.03.1996	07.2000

Note. D is diameter, mm; s is thickness, mm.

Table 2. **Results of inclination measurements of the deformed segment of Well 8032**

Depth interval, m	Drift angle, degrees		Note
	Open hole*	Production string**	
0–100	0	1.00	
100–229	0	1.00–6.45	
230–239	0	8.00–11.45	Interval of building curvature (casing bulging)
240–246	0	8.30–3.45	Interval of curvature decline
247–252	0	13.15–17.30	Interval of maximum curvature (casing bulging)
253–259	0	16.45–5.45	Interval of curvature decline (data from tubing)
260–266	0	2.30–2.15	Almost straight hole (data from tubing)
266–300	0.15	1.30–0.45	Straight hole (data from tubing)
300–500	0.15	0.15–1.00	Straight hole (data from production string)

* Date: 04.01.1995.
** Date: 20.08.2000.

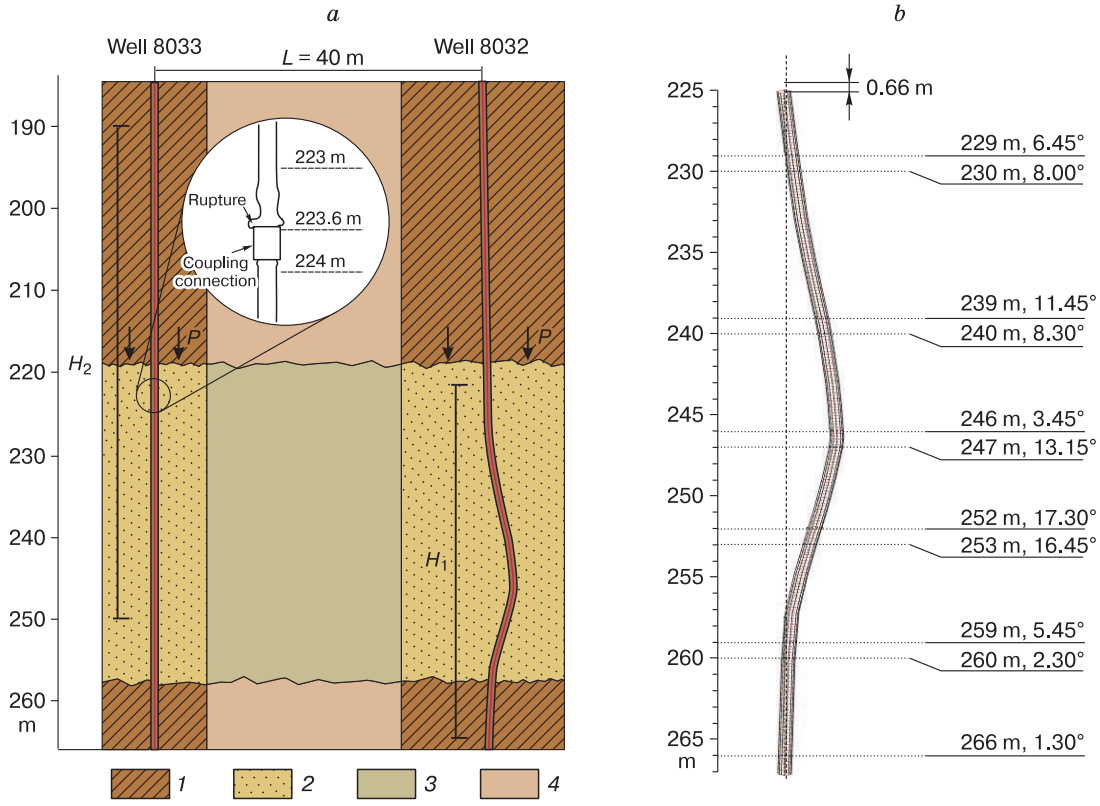

Fig. 1. Conditions and mode of the deformations of wells, the Yamburg GCF:

a – geological section and mode of deformations of Wells 8032 and 8033; *b* – detailed information on the deformed segment of Well 8032, the Yamburg GCF (inclination measurement data as of 20.08.2000), values of drift angle of a local segment of the wellbore casing from vertical plane; *1* – unfrozen compacted clay; *2* – unfrozen weakly consolidated sand; *3* – frozen sand; *4* – frozen clay.

wthin this depth interval. The tubing string deflection (buckling) was reported in the 216.5–226.5 m depth interval.

The depths denoted as H_2 and H_1 indicate deformed intervals of Wells 8033 and 8032, respectively. The deformation in Well 8032 was reported from the 225–268 m interval, i.e. the length of H_1 interval is 43 m, while the H_2 deformation interval in Well 8033 measures about 60 m and is located at a depth between 190 and 250 m. With the deformation intervals and depths of both wells being roughly equal, and given the distance between the wells is 40 m, we can infer that the cause of deformation resides in the structural geology of permafrost deposits and their thawing properties.

1.2. The Vankor field. On one of the well pads of the Vankor field, likewise in the Yamburg GCF, the buckling was reported from two nearby wells (with their subsequent forced shutdown). The actual data on these wells were presented by company "Vankorneft" at the November 2015 back-analysis workshop on the deformations occurred, (with the participation of the MPI SB RAS specialists). The design and technological parameters of the deformed wells are listed in Table 3. Fig. 2 presents a three-dimensional view of the deformed areas and depth intervals with respect to their placement within the rock mass. The maximal deformation of both wells is confined to the depth range from 170 to 195 m. The deformed segments of both wells exhibited deformation in the form of corrugated folds, which was probably due to the effect of axial force causing metal yield (plastic deformation). No deflection of vertical position of the wellbore casing was observed within the deformation interval. No more detailed geological information on permafrost in the Vankor field area is available.

1.3. Exxon Laboratory experimental data in comparison with field observations. At the end of the 1980s, Exxon company conducted a series of experiments for the study of effects of axial compressive loads on model surface casing of different diameters and lengths [*Hirshberg et al., 1988*]. The aim of the experiment was to analyze the effect of vertical loads on the surface casing arising from the permafrost thaw subsidence during the production life of wells in oil and gas fields of Alaska. The study includes the data on the pipe material properties and characteristics of sample loading conditions. The laboratory

Table 3. **Design and technological parameters of the deformed wells, the Vankor field**

Well	$D \times s$		Period of drilling conductor hole	Commissioning date	Shutdown date	Further details
	Conductor (surface casing)	Production string				
1	245 × 8.9	178 × 10.4	11–18.08.2008	10.08.2009	08.09.2013	Permafrost thawing and caving formation while drilling. Height of cement lift in behind the surface casing is 182 m from wellhead
2	245 × 8.9	178 × 10.4	04–08.08.2008	29.01.2010	08.09.2015	Permafrost thawing and caving formation while drilling. Height of cement lift behind the surface casing is 191 m from wellhead

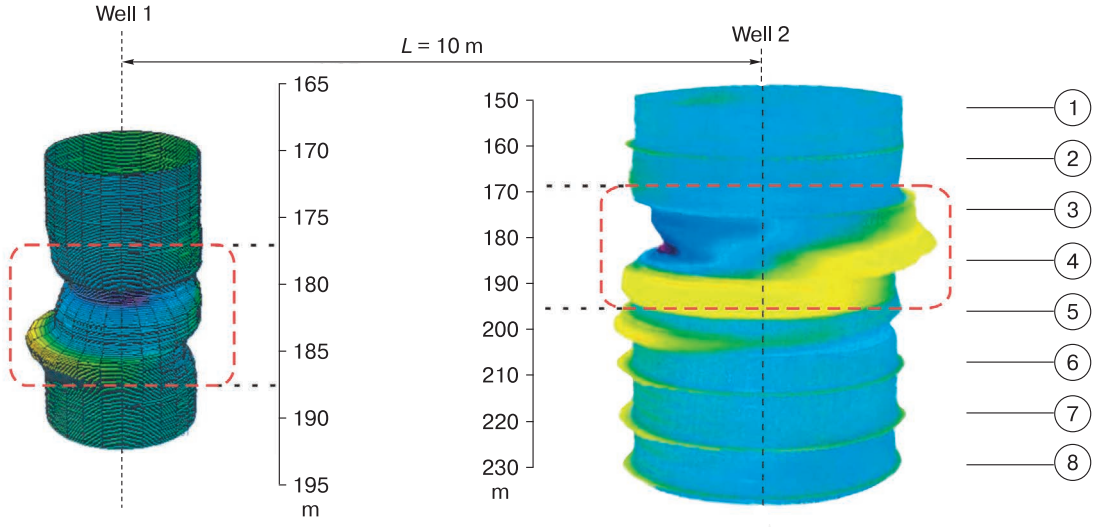

Fig. 2. Fragments of wellbore casing deformations, the Vankor field (instrumental measurement data).

Depth scale for the deformations interval, m; 1–8 – numbering for coupling connections in the deformations interval; the red dotted lines accentuate localities of maximum deformations.

sample, in itself, consisted of two sections of a casing tube joined by coupling connections (Fig. 3). The sample in Fig. 3, *a*, *b* is shown in two states – prior to and after the application of failure load. The photo in Fig. 3, *c* shows a lengthwise cut of the deformed segment of the model on the contact with the coupling. During testing, all samples were similarly deformed, namely with the formation of a circumferential bulging (ridges) on one side of the coupling surface. Subsequent compression which inflated the bulging, eventually bended the coupling, culminating in a rupture of the pipe body. The authors' observations indicate that, when approaching the failure point, the encasement material manifested remarkably plastic behavior. Note that the failure load in the discussed experiments reached the values of about 8 Meganewtons (MN) (i.e. 800 tnf).

A comparative analysis of strain capacities of casing strings at the Yamburg (Well 8033) and Vankor fields and deformations of samples in the laboratory compression test has revealed common features in the behavior of resulting deformations.

1. Likewise in the laboratory experiments, the deformation of casing strings observed at producing wells involved the formation of circumferential bulging (ridges), which was underpinned by strain-gauge data on the deformed interval of casing strings.

2. The circumferential bulging forms on the pipe segments tightly adjacent to the coupling connection, while physical compression tests have shown that the deformation occurs only on one side of the coupling surface. The more so, this specific feature of deformation is observed in three of the four cases of deformation of production wells in the investigated oil fields.

3. The yellow indicator light and corresponding levels of the deformation zones in the casing string in Fig. 2 clearly indicate that a spacing between the ridges formed is approximately 11.5 m, which is equal to the length of the casing segments and fits in with the position of the coupling connections.

With the above considerations in mind concerning the laboratory simulation of the axial load effects on the casing, and the results of previous calculations of loss of axial stability [*Gorelik and Soldatov, 2016*], one can infer that all of the discussed deformations of casing strings both at the Yamburg and Vankor fields have resulted from high axial loads on the wellbore casing.

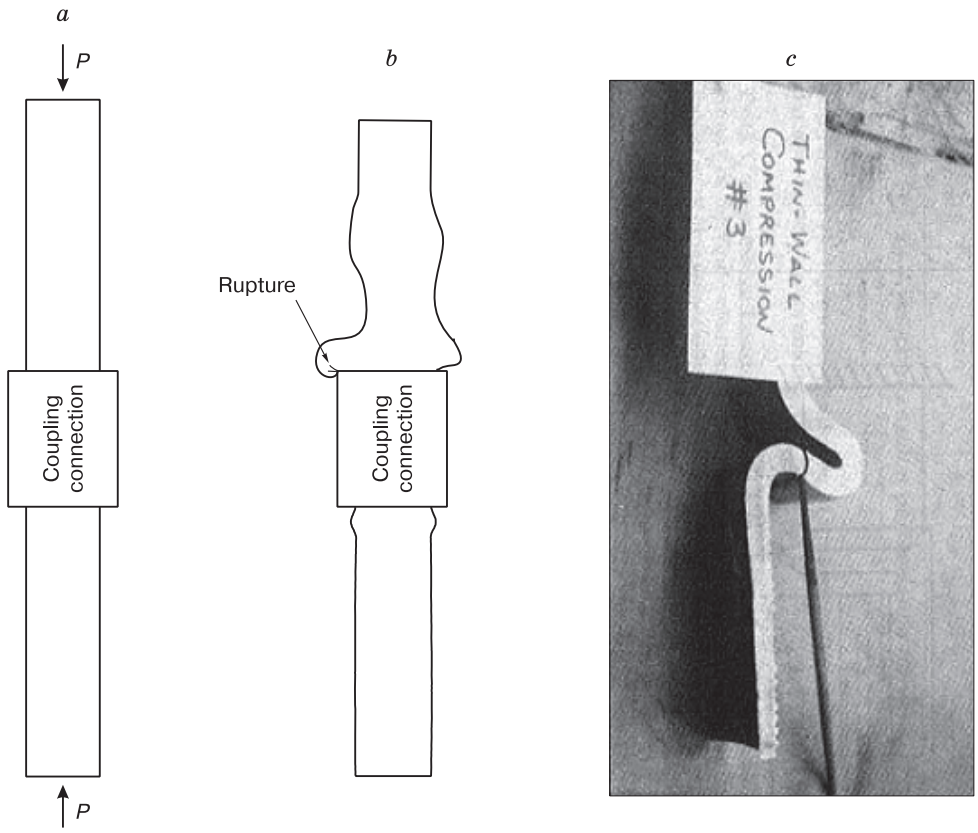

Fig. 3. The test sample of a casing tube:

a, *b* – schematic representation prior (*a*) and after (*b*) the axial fail load test; *c* – photograph of the longitudinal cut of the deformed section of casing tube [*Hirshberg et al., 1988*].

2. Calculation of axial loads on the wellbore casing contributed by thawing permafrost

2.1. Introductory notes. The safety design criteria for wells capable of withstanding emerging loads requires an adequate method for their calculation. An overview of existing approaches to this problem is given in [*Gorelik and Soldatov, 2016*]. Within the scope of this research, we will limit ourselves to briefly mentioning a study [*Goodman, 1978*], which provides theoretical explanation of emerging additional loads on wellbore casing during thawing of permafrost, proceeding from the assumption of zero pore pressure in the thawing soils. However, given that the assumption provided in [*Goodman, 1978*] lacks a description of processes and situations leading to such inferences, it therefore cannot be accepted without respective investigations to prove the disappearance of hydrostatic pressure in some instances.

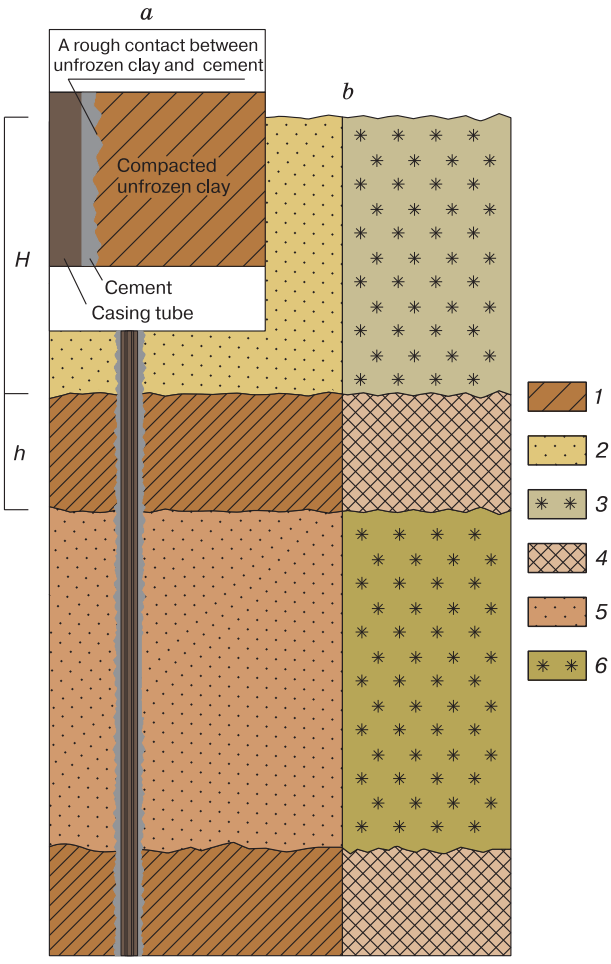

Fig. 4. Illustration for selection of a calculation scheme:

a – clayey bed – cement sheath adhesion boundary; *b* – geological section; *1* – compacted unfrozen clay; *2* – unfrozen sand; *3* – frozen sand; *4* – compacted frozen clay; *5* – unfrozen compressible sand (elastic subgrade resistance); *6* – frozen soil.

In [*Gorelik and Soldatov, 2016*] the empirical relation from [*Bratsev and Zhukov, 1965*] for the axial force of negative friction P_{sh}, affecting the wellbore casing at a depth H, which is used in the design of mine shafts in permafrost has the following form:

$$P_{sh} = \pi a R \rho g H, \qquad (1)$$

где ρ is density of unfrozen soil; a, R is both the outer external cement sheath radius and current value of the thaw radius; $g = 9.81$ m/s^2. Importantly, expression (1) takes into account the current position of the thaw radius, implying that this forcing is time-dependent. At this, the authors emphasize that the dependency of negative friction from the thaw radius is clearly traced only to its propagation to 4–5 m, and then becomes unfeatured (i.e., the value of more than 5 m in (1) necessitates the substitution of $R = 5$ m).

In fact, this means that the impact of the thaw radius can be material only during first years of the facility operation. However, the underlying theory of this formula is rather vague, and so is its applicability. The described below method for obtaining an alternative ratio, taking into account the geological structure of rock mass hosting the well and their physical and mechanical properties in thawing and unfrozen state.

2.2. Geological prerequisites for the calculation scheme. Geological sections of the target oil/gas field areas residing within the permafrost interval are composed by interbedded clayey and sand-loamy layers of different thickness [*Baulin et al., 1967; Dubikov, 2002*]. Geocryological characteristics of the Yamburg GCF are provided in [*Gorelik et al., 2015*]. The discussed below calculation scheme largely relies on the specific properties of individual beds (Fig. 4).

These are as follows for *sands*: a) sands in the unfrozen state have no adhesion between their particle and therefore are unable to transmit the weight load of all their thawed mass onto vertical walls of the wellbore casing; b) when thawing, their consolidation proceeds fairly quickly under the action of their own weight as the excess moisture is squeezed out; for *clays*: a) clayey beds in the unfrozen state may have sufficiently high strength and until the thaw radius has reached a certain value are capable of resisting the weight of the overburden without collapsing (caving-in), while experiencing some subsidence (under the condition of water draining from the underlying soils outside the limit of their extent); b) cave-in deformations inevitably cause a force reaction of the underlying sandy soil (directed opposite to gravity), whose quantitative description can be given within the scope of known mechanical models (for example, an elastic subgrade resistance); c) the unfrozen part of the clayey bed expands along its outer boundary into the frozen rock, whereas along the inner boundary, it is connected with a rough wall of the outer cement ring of wellbore casing whose radius (with respect to depth) is close the average value (Fig. 4, *a*).

Note that despite the information available from technical reports for the Yamburg GCF emphasizing the higher structural strength and other mechanical characteristics of frozen clays identified in some beds, the data describing those same rocks in the unfrozen state are not available.

2.3. Calculation scheme and method. These properties of individual formations allow interpreting the unfrozen portion of the clayey bed as a slab residing on an elastic foundation, which is subject to caving-in under the action of the overburden weight and the force reaction of the underlying thawed soils with the specified constraining condition for both boundary contours as a computational model for calculating the load on the wellbore casing. A simple type section shown in Fig. 4, which includes a single clay layer is discussed below.

More complex cases of sections composed by several clayey layers require generalization of the calculations given below and are not considered here. Suppose that H is the occurrence depth of the top of clayey bed and its thickness is denoted by h. The layer has the form of a round slab with an external radius R_2 (equal to the current value of the thaw radius) and a round hole in the center of radius R_1 (equal to the average value of the radius of the outer cement ring). We denote E, σ as elasticity modulus o and Poisson's ratio for clays, while D is cylindrical stiffness of the slab. At this

$$D = Eh^3 \Big/ \left(12\left(1-\sigma^2\right)\right). \qquad (2)$$

Elastic resistance of the underlying soil will be described by the ratio of the elastic subgrade resistance

$$p_w = kw, \qquad (3)$$

where p_w is reactive pressure; w is the value of vertical deformation of the slab; k is the coefficient of subgrade resistance. If the external load q applied to the slab is axisymmetric with respect to its central axis, then the static deformation of the slab in the cylindrical coordinate system depends only on the radial coordinate r and is described by a non-uniform biharmonic equation [*Korenev, 1954; Timoshenko, 1967*]. These works introduce dimensionless quantities and the parameter having dimensionality of length l:

$$u = w/l,\ x = r/l,\ Q = ql^3/D,\ l = \sqrt[4]{D/k}. \qquad (4)$$

Then the equation is written in a dimensionless form:

$$\Delta_x \Delta_x u + u = Q; \qquad (5)$$

$$\Delta_x = \frac{d^2}{dx^2} + \frac{1}{x}\frac{d}{dx}. \qquad (6)$$

As is the case here, the external load q is determined from the weight of the overlying soil mass (including the weight of the clayey bed) minus the water force and is written as:

$$q = \left(\rho_s - \rho_w\right) g(H+h), \qquad (7)$$

where ρ_s, ρ_w are soil density in the unfrozen state and density of water; g is acceleration of gravity. As defined by expression (7) the load q is independent from the radial coordinate (i.e. constant along the radius). The account of the water force in (7) is valid if at intermediate stages of consolidation the water can drain from the underlying clayey layer of soil to the overlaying soils through gaps and cracks on the contact between the clayey layer and cement, up until its stabilized condition in which deformations are described by equation (5).

The conditions of rigid clayey formation sealing along the outer and inner perimeters of the slab are assumed as boundary conditions for (5), which leads to the four additional conditions:

$$u\left(x_1\right) = u\left(x_2\right) = 0,\ \ u'\left(x_1\right) = u'\left(x_2\right) = 0, \qquad (8)$$

where $x_1 = R_1/l$; $x_2 = R_2/l$; the slash stands for the x-derivative.

Equation (5) is the fourth-order linear nonhomogeneous differential equation. Its general solution is defined by the sum of the general solutions of the homogeneous part (at $Q = 0$) and any of the particular solutions (5). The general solution of the homogeneous part is expressed by the linear combination of four Bessel functions: ber(x), bei(x), ker(x), kei(x) [*Timoshenko, 1967*] (aka Kelvin functions [*Abramovits and Stigan, 1979*]). At Q = const the particular solution (5) is the function $u(x) = Q$. Thus, the general solution (5) can be presented as

$$u(x) = Q + A_1\,\mathrm{ber}(x) + A_2\,\mathrm{bei}(x) + \\ + A_3\,\mathrm{ker}(x) + A_4\,\mathrm{kei}(x). \qquad (9)$$

The unknown constants A_1–A_4 are defined from the conditions of (8) (being way too cumbersome, the expressions are not given here). If we assume that the value x_1 is fixed, then each of these constants is the function of three input parameters: Q, l, x_2. A method for their explicit definition shows that each of these functions can be represented as follows:

$$A_n = Q\,\varphi_n(l, x_2),\ n = 1, 2, 3, 4, \qquad (10)$$

where φ_n functions are invariant with Q.

The sum of force reactions on the inner (P_i) and outer (P_e) contours of the slab are determined by the known expressions [*Korenev, 1954; Landau and Lifshits, 1987*]

$$P_i = 2\pi R_1 \frac{D}{l^2}\frac{d}{dx}\Delta_x u_{x=x_1}; \qquad (11)$$

$$P_e = -2\pi R_2 \frac{D}{l^2}\frac{d}{dx}\Delta_x u_{x=x_2}. \qquad (12)$$

Given (9) that the application of the Laplace operator indicated in the parentheses in (11) and (12) to any of Kelvin function translates it to another function from the same group with the respective sign [*Abramovits and Stigan, 1979*] (for example,

$\Delta_x \operatorname{ber}(x) = -\operatorname{bei}(x)$, etc.), these relations can be rewritten through the first derivatives of Kelvin functions. In particular, for the internal contour (on the contact with wellbore casing) we obtain

$$P_i = 2\pi R_1 \frac{D}{l^2}\left(-A_1 \operatorname{bei}'(x_1) + A_2 \operatorname{ber}'(x_1) - A_3 \operatorname{kei}'(x_1) + A_4 \operatorname{ker}'(x_1)\right). \quad (13)$$

Proceeding from the ratios (4), (10), (13), it can be easily demonstrated that the dependence of P_i (as well as P_e) values on the parameters of E and k is reduced to the dependence only on their ratio (E/k). This property can reduce the amount of calculations required. By multiplying both parts of equation (5) by x and integrating them in the range from x_1 to x_2, as well as for the central angle in the range from 0 to 2π, we obtain the equation for the integral balance of forces acting on the slab in the state of its mechanical equilibrium. It can be represented as

$$P_i + P_e + P_w = -P_q, \quad (14)$$

where P_i, P_e are defined by equations (11) and (12); P_w is the total elastic subgrade resistance, given by the formula

$$P_w = 2\pi \int_{R_1}^{R_2} p_w(r) r dr = 2\pi k l^3 \int_{x_1}^{x_2} u(x) x dx, \quad (15)$$

P_q – total load from the overburden weight:

$$P_q = \pi l^2 q\left(x_2^2 - x_1^2\right). \quad (16)$$

Equation (14) is convenient to use as a test relation for the calculations performed.

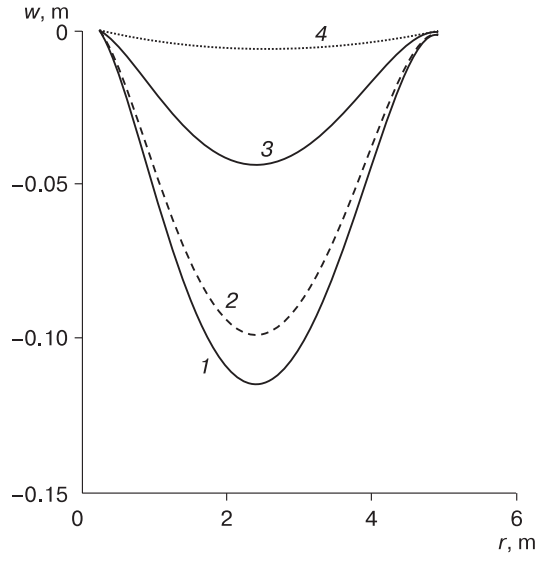

Fig. 5. Plot of vertical deformations of the formation (w) versus radial coordinates (r) at R_2 = 5 m and different values of k:

1 – 10^3 Pa/m; *2* – 10^6 Pa/m; *3* – 10^7 Pa/m; *4* – 10^8 Pa/m.

Note that instead of the set of functions selected in (9), B.G. Korenev and his associates [*Korenev, 1954; Korenev and Chernigovskaya, 1962; Gorbunov-Posadov et al., 1984*] use a different set (linked with Kelvin functions by linear relations), which required compiling special tables. However, the set of functions used here, has significant advantages, consisting in high-precision interpolation expressions for them (as well as for their first derivatives) [*Abramovits and Stigan, 1979*], which allowed to make the process of calculations largely automated.

The transition to the dimension values is carried out through the ratios of (4). If the axis Ow is directed upwards, the w, g и P_q values are negative (since the cave-in deformations, the gravity and the weight of soils are directed downwards, i.e. opposite to the direction of the axis Ow), whereas reaction forces (P_i, P_e, P_w) in (14) therefore must be positive (they are directed upwards).

Formulas (9), (11), (12) with the account of (13), (15), (16) allow to calculate all necessary values characterizing the equilibrium state of the clayey slab and the corresponding reactive forces in all the system's elements. With regard to well design, the most important is the calculated load exerted onto the wellbore casing (the total reaction force in the slab P_i inner fastening contour) and its dependence on the thawmradius.

However, other values may be useful in assessing the effects of the related processes (e.g., in the analysis of subsidence of the thawing soil, for establishing the magnitude of loads ensuring integrity of the clayey formation, etc.).

2.4. Calculation examples. Let us consider examples of calculations for different values of the subgrade resistance coefficient (covering the range of possible values of this parameter for unfrozen soils [*Korenev and Chernigovskaya, 1962*]) given the following input data: H = 70 m, h = 2 m, R_1 = 0.2 m, $E = 10^7$ Pa, $\sigma = 1/6$, $\rho_s = 1800$ kg/m^3, $\rho_w = 1000$ kg/m^3, and for different values of thaw radius R_2. The elasticity modulus E is assumed to be close to this factor for clays with highest densities. All the calculations are easily carried out in the MathCad environment.

Figure 5 represents the results of calculations of the clay slab deformation at a fixed value of thaw radius R_2 = 5 m and different values of the subgrade resistance coefficient. Note that when the coefficient of subgrade resistance changes by five orders of magnitude, the maximum curvature changes by about an order of magnitude.

Table 4 provides a calculus example for relationship between the total load coupled with all reaction forces and the value of thaw radius. Using Table 4, the accuracy of calculations can be estimated from ratio (14). For comparison, the last column shows the dependence of the load on the casing, defined by

Table 4. **Total loading and reaction forces (absolute values) versus the position of thaw radius (R_2) at $k = 10^7$ Pa/m**

R_2, m	P_i	P_e	P_w	P_q	P_{sh}
	tnf				
0.2	0	0	0	0	15
0.5	14.4	22.8	0	37.2	38
1.0	55.1	115.1	0	170.2	77
1.5	116	273.5	2.2	392	116
2.0	195	493	14	702	155
2.5	284	760	57	1101	194
3.0	371	1053	165	1589	233
3.5	441	1344	380	2165	271
4.0	486	1613	731	2830	310
4.5	503	1856	1225	3584	349
5.0	500	2078	1848	4426	388
6.0	470	2498	3408	6377	465

Note. For illustrative purposes, all load bearing characteristics (P_i, P_e, P_w, P_q, P_{sh}) are given in ton-force (1 tnf = 10^4 N). See text for detailed notations (equations (11), (12), (15), (16), (1)).

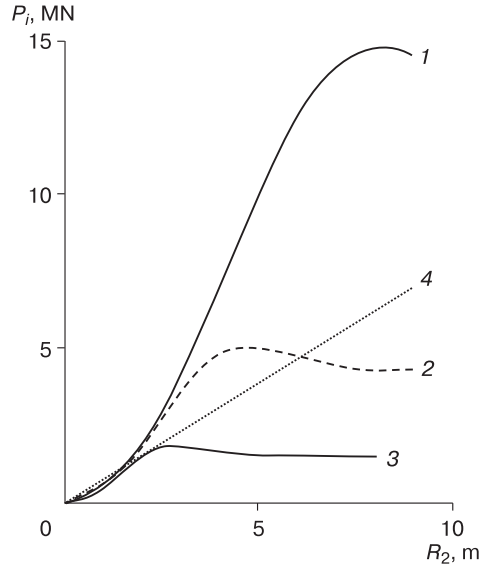

Fig. 6. Relationship between total loads on wellbore casing (P_i) and thaw radius (R_2) at and different values of k:

1 – 10^6 Pa/m; *2* – 10^7 Pa/m; *3* – 10^8 Pa/m; *4* – from equation (1).

equation (1). This example shows variations in monotonous behavior of the load exerted on the casing within the range of the thaw radius from 4.5 to 6 m.

Figure 6 shows the behavior of total load on the wellbore casing depending on the thaw radius at three values of the subgrade resistance coefficient. The load curve obtained by the calculation using formula (1) is given here for comparison.

2.5. Discussion of results. In contrast to equation (1), the proposed calculus method demonstrates a non-monotonic dependence of the load on the thawing radius. At the initial stage, the load increases to a certain maximum value, followed by it decreasing until it becomes an asymptotically constant (independent from R_2) value. The value of the maximum and the asymptotic value decrease with the growth of the coefficient of subgrade resistance (with the response of foundation P_w being critical in the redistribution of reaction loads). The position of the maximum is shifted towards larger R_2 values as the subgrade resistance coefficient decrease (i.e., with decreasing resistance of the elastic foundation, the maximum load corresponds to the later moments of time from the commencement of well operations). For example, for coefficient $k = 10^3$ Pa/m, a peak on the curve is equal to about $6 \cdot 10^7$ N (6000 tnf). At this, its position approximately corresponds to the value of $R_2 = 13$ m, which normally occurs after several decades of continuous well operations. However, these loads reach collapse values already at the thaw radius of 5–6 m (at a rated depth of 70 m). Low k-values can be characteristic of soils with higher ice content in the initial (permafrost) state. In this case, the loads exceed the failure values used in the experiments [*Hirschberg et al., 1988*], which is also hazardous in terms of loss of axial stability of the wellbore casing [*Gorelik and Soldatov, 2016*]. Soils which become highly consolidated in the process of formation, followed by their epigenetic freezing and having therefore high strain resistance factors, are safer for well operations. We should however bear it in mind that the calculated loads (given (10) and (13)) are actually proportional to the occurrence depth of clayey formation H, which means that for a depth of approximately 200 m (at which the accidental buckling of wells was reported), the peak loads will reach hazardous values, including the coefficients of subgrade resistance $k = 10^7$ and 10^8 Pa/m.

The load behavior shown in Fig. 6 is fully consistent with the observed in situ effect of the thawing process on the timing and magnitude of deformations of the wellbore casing [*Bratsev and Zhukov, 1965*] and wells [*Gorelik et al., 2015*]. The first few years have proven to be most hazardous for the structures since their commissioning, while further operation reduces the risk of hazardous deformations.

The presence of a peak in function $P_i(R_2)$ is not obvious, and it would be pertinent to give some physical reasoning for its justification. The parameter l, introduced by the ratios in (4), estimates a typical distance from the point of local load application to the slab at which its deformations are tending to decline until a certain constant value is reached. For example, if the main focus is on the solution of the

problem of infinite slab deformed under the action of concentrated force, then this distance approximately equals 3*l* [*Timoshenko, 1967*].

In the considered problem, local (nonuniform) loads are localized on the circular contours of the slab. If the slab radius R_2 is large enough to have the condition $R_2 >> 2(3l)$ satisfied, the pattern of the slab deformations (in the transverse section) should have a saucer-like shape: the extended bottom is limited from the edges by fairly sharply rounded elevations whose length along the radius approximately equals 3*l*.

Both the shape and characteristic dimensions of the elevations will be slightly dependent on the bottom's length when fulfilling the written inequality and at progressively increasing R_2. This means that at a fixed value of R_1, the function $P_i(R_2)$, according to (11), asymptotically tends to a constant value. At the same time, according to (12), the function $P_e(R_2)$ should increase linearly under the same conditions.

In this case, the total load of the overburden weight (which, according to (16), is proportional to $(R_2)^2$) is compensated primarily by the reaction of the elastic base (as follows from (15), it is also proportional to $(R_2)^2$). At this, it is obvious that with the R_2 increasing from the value of R_1, at least in the close vicinity of this point, all reactive forces being proportional to the weight of the overlying deposits should increase.

The insights resulting from the above considerations indicate that as the value of R_2 increases, the load exerted on the wellbore casing should increase monotonously at the initial time of permafrost thawing and it tends to be an asymptotically constant value at long term operations. This, however, does not yet unambiguously necessitate the existence of a maximum in this function behavior (which is possible only if the asymptotic value is approximated from above). Taking into account that the relationships between the A_1–A_4 coefficients and that variable R_2 is too cumbersome, the actual presence of this maximum is defined purely by calculations. The proposed calculation method allows to closely approach the optimal solution to the problem of convergence of the wellheads within a well pad in the permafrost proceeding from the condition of ensuring stability of wells during operation.

It should also be noted that this calculation method requires sufficient information about the alternation pattern of clay and sandy soil layers within the permafrost interval and their deformation characteristics in the unfrozen state.

CONCLUSIONS

1. The known facts of forced shutdown of wells at high-latitude hydrocarbon fields clearly demonstrate the effect of additional loads on the wellbore casing resulting from permafrost thawing. The laboratory (experimental) studies of the action of these loads on the casing models have shown that the load can exert failure strain of two types: loss of axial stability of the wellbore casing; plastic flow of metal elements of the casing on the coupling connection surface associated with the bulging. The greatest challenge in designing structurally stable wells for permafrost areas consist in the development of appropriate method for calculating axial loads on the well bore casing, stemming from the permafrost thawing during the production life of wells.

2. The discussed approach to calculating vertical loads suggests that they are communicated by the weight of thawing soils, overlying the steadfast clay layers, residing on the inner contour of the well casing and extending along its outer contour into the permafrost not affected by thawing; whereas from below, they are exposed to elastic reaction of the underlying soils in the unfrozen state.

3. With the permafrost thawing around the well, the loading on the wellbore casing reveals (unlike the known approaches) the non-monotonous behavior with the increasing thaw radius. At first, the load increases to a certain maximum value, which then decreases until it becomes asymptotically constant value (independent from of R_2). The maximum and the asymptotic values of the loading tend to decrease, as the subgrade resistance coefficient grow. When decreasing, this coefficient is reflective of a shift in the position of the maximum towards larger R_2 values. At low values of the failure strain coefficient ($<10^5$ Pa/m) the values of these loads reach already at the thawing radius of 5–6 m (at the clay occurrence depth of 70 m).

4. Low values of coefficient *k* can be indicative of ice-rich permafrost. In this case, the loads exceed the failure strain values, which were reported in the experiments [*Hirschberg et al., 1988*], and are also hazardous for loss of axial stability (buckling) of the wellbore casing [*Gorelik and Soldatov, 2016*]. Soils, highly consolidated in the process of their formation, epigenetically frozen and having high coefficients of resistance to deformation, appear essentially safer for well operations. For a depth of about 200 m (at which accidental deformations of wells were reported) the load at the maximum point will reach hazardous values, including for the coefficient of subgrade resistance $k = 10^7$ and 10^8 Pa/m.

5. As is shown in Fig. 6, the behavior of the loading exerted on the wellbore casing is consistent with the *in situ* observations of the effects of permafrost thawing on the duration and intensity of deformations in mine shafts [*Bratsev and Zhukov, 1965*] and wellbore casing [*Gorelik et al., 2015*]. In this respect, the first few years from their commissioning are the most hazardous for the facilities. Further operations reduces the risk of emerging hazardous deformations.

The authors express their gratitude to the reviewers Professor L.N. Khrustalev, Dr. sci. eng., Professor V.G. Griguletsky Dr. sci. eng., for careful reading of the manuscript and valuable comments; to the management of "Gazprom Yamburg" Company for the interest and assistance in the research; to Deputy Director General of "TyumenNIIgiprogaz" Company Cand. sci. eng., V.F. Shtol for his interest and helpful advice.

The work was supported by a grant of the President of the Russian Federation for leading scientific schools (HIII-3929.2014.5).

References

Abramovits, M., Stigan, I. (Eds.), 1979. Manual of Special Functions. Nauka, Moscow, 831 pp. (in Russian)

Baulin, V.V., Belopukhova, E.B., Dubikov, G.I., Shmelev, L.M., 1967. Geocryological Conditions of the West Siberian Lowland. Nauka, Moscow, 214 pp. (in Russian)

Bratsev, L.A., Zhukov, V.F. (Eds.), 1965. Theory and Practice of Permafrost Science in Construction. Nauka, Moscow, 188 pp. (in Russian)

Bykov, I.Yu., 1991. Environmental Protection in the Extreme North upon Borehole Drilling. Izd-vo LGU, Leningrad, 238 pp. (in Russian)

Dubikov, G.I., 2002. Composition and Cryostratigraphy of Permafrost in Western Siberia. GEOS, Moscow, 246 pp. (in Russian)

Goodman, M.A., 1978. World Oil's Handbook of Arctic Well Completions. Gulf Publ. Company, Houston, Texas, USA, 51 pp.

Gorbunov-Posadov, M.I., Malikova, T.A., Solomin, V.I., 1984. Design of Structures on Elastic Foundation. Stroiizdat, Moscow, 680 pp. (in Russian)

Gorelik, J.B., Soldatov, P.V., 2016. Instability of casing in permafrost production wells with a lateral support from thawing ice-rich soil. Earth's Cryosphere XX (4), 84–92.

Gorelik, J.B., Soldatov, P.V., Seleznev, A.A., 2015. Thermal stability of frozen ground at sites of well clusters in the Yamburg gas-condensate field. Earth's Cryosphere XIX (1), 53–60.

Hirshberg, A.J., Moyer, M.C., Rickenbach, R.M., 1988. Surface-casing strain capacity for north slope operations. SPE Drilling Eng., Sept., pp. 289–295.

Korenev, B.G., 1954. Problems of Designing Beams and Slabs on Elastic Foundations. Gosstroiizdat, Moscow, 232 pp. (in Russian)

Korenev, B.G., Chernigovskaya, E.I., 1962. Analysis of Plates on Elastic Foundations. Gosstroiizdat, Moscow, 356 pp. (in Russian)

Landau, L.D., Lifshits, E.M., 1987. Course of Theoretical Physics, Pt VII. Theory of Elasticity. Nauka, Moscow, 248 pp. (in Russian)

Medvedskiy, R.I., 1987. Construction and Operation of Petroleum Wells in Permafrost. Nedra, Moscow, 230 pp. (in Russian)

Remizov, V.V., Kononov, V.I., Bereznyakov, A.I., et al., 2001. Nadymgazprom: Geotechnical Monitoring in Permafrost. IRC Gazprom, Moscow, 149 pp. (in Russian)

Timoshenko, S.P., 1967. Stability of Rods, Plates and Shells. Nauka, Moscow, 620 pp. (in Russian)

Vasilevsky, V.V., 2002. Improving operation reliability of gas and oil wells in permafrost: Extended abstract of Cand. Sci. (Techn.) dissertation. Moscow, 2002, 163 pp. (in Russian)

Vyakhirev, R.I. (Ed.), 1996. Improving the system for gas fields development and operation in the Extreme North, Nauka, Moscow, 406 pp. (in Russian)

Received May 22, 2017